Arabian Journal for Science and Engineering (2018) 43:7209–7218
https://doi.org/10.1007/s13369-017-3057-2

RESEARCH ARTICLE - COMPUTER ENGINEERING AND COMPUTER SCIENCE

Iris Recognition Using Zernike Moments and Polar Harmonic Transforms

Bineet Kaur[1] · Sukhwinder Singh[1] · Jagdish Kumar[2]

Received: 1 June 2017 / Accepted: 21 December 2017 / Published online: 9 January 2018

Abstract
Iris recognition in uncontrolled environment acquired in different domains (cross-spectral and cross-sensor) poses a challenge for being considered for high-security applications. In this paper, a feature-set invariant to rotation, noise and illumination is proposed consisting of Zernike moments and polar harmonic transforms. Each of these is extracted from localized iris regions till 15th order on five publicly available databases: CASIA-IrisV4-Interval, IITD.v1, UPOL, UBIRIS.v2 and IIITD-CLI. The proposed method proves to be effective for near-infrared and visible images collected from different iris sensors, thus giving a superior performance as compared to existing techniques available in the literature in terms of receiver operating characteristic curve, accuracy, equal error rate and decidability index.

Keywords Biometrics · Iris recognition · Orthogonal moments · Polar complex exponential transform · Polar cosine transform · Polar sine transform · Zernike moments

1 Introduction

Biometric systems are used for identifying a person on the basis of his/her behavioral and physiological traits. Among these, iris is the most reliable modality based on its unique texture, stability throughout lifetime and easy accessibility. Biometric systems based on iris have been implemented in various practical applications like the Aadhaar project [1] in India for recognizing millions of citizens and UAE border crossing application [2]. Researchers have reported remarkable results for iris images collected using near-infrared (NIR) imaging in controlled environment. However, to make these systems desirable for high-security applications certain limitations like images acquired at a distance under uncontrolled environment using different sensors and imaging wavelengths need to be overcome.

1.1 Related Work

Most of the researchers have implemented algorithms on NIR imaging taken under controlled environmental conditions. Daugman for the first time implemented an iris recognition system using integro-differential operator for iris segmentation, 2D Gabor filter for iris encoding and hamming distance for matching [3]. Bhateja et al. [4] proposed sparse representation with compressive sensing and k-nearest subspace using genetic algorithm for classification which gave zero false acceptance ratio (FAR). Liu et al. [5] used Gabor filters and scale-invariant feature transform (SIFT) key points with support vector regression which outperformed existing approaches on NIR images. Umer et al. [6] implemented restricted circular Hough transform (RCHT) for iris segmentation with multi-scale morphological features which gave superior results in comparison with recent approaches. Rai et al. [7] implemented iris recognition using support vector machine (SVM) and hamming distance along with Haar wavelets and log-Gabor filters which gave outstanding results for NIR images. Images collected in visible range suffer from specular reflections from nearby objects in addition to eyelid and eyelash occlusion. Umer et al. implemented a robust iris

✉ Bineet Kaur
bineetkaur91@gmail.com

Sukhwinder Singh
sukhwindersingh@pec.ac.in

Jagdish Kumar
jagdishkumar@pec.ac.in

[1] Department of Electronics and Communication Engineering, Punjab Engineering College (Deemed to be University), Chandigarh, India

[2] Department of Electrical Engineering, Punjab Engineering College (Deemed to be University), Chandigarh, India

recognition system based on sparse representation coding by spatial pyramid Mapping using modified BioHashing method for feature extraction which proved to be effective for NIR and visible databases [8]. Alvarez-Betancourt et al. proposed detectors for key points identification of SIFT features—Harris-Laplace, Hessian-Laplace and Fast-Hessian which proved to be robust for NIR and visible images [9]. Tan et al. [10] implemented Zernike moments which were phase-encoded for both NIR and visible images.

1.2 Motivation and Proposed Work

The availability of different iris sensors acquiring images under varying wavelengths degrades the performance of an iris recognition system. The cross-domain problem arises when images collected in one domain (sensor-specific and wavelength-specific) are matched against another domain. Thus, working on cross-domain iris recognition poses a challenge as opposed to NIR-based systems that are void of such noise factors. The objectives of the paper are as follows:

1. To develop a robust method that works on NIR and visible images using different iris sensors under less constrained environment.
2. To extract features that can perform well for cross-domain iris recognition problem. For this, a novel method is developed by constructing an orthogonal feature-set with rotation, noise and illumination invariance consisting of Zernike moments, polar cosine transform, polar sine transform and polar complex exponential transform extracted on localized iris texture regions.
3. To select an optimum combination of moment order and number of features that contains adequate information for iris texture classification.
4. To analyze and compare the performance of the proposed method with recent approaches on various publicly available databases.

2 Proposed Methodology

The proposed methodology used for iris recognition system is discussed in the following section along with illustration shown in Fig. 1.

2.1 Iris Segmentation

The process includes localization of the pupil–iris and iris–sclera boundary of human eye. For iris segmentation, circular Hough transform (CHT) has been used which is insensitive toward noise and detects circular objects in an image [11]. Each edge point is assumed as the centre, and circles are drawn at varying radii. The pixels lying on the perimeter of the circle are stored in an accumulator. Iris being the largest part of the human eye will have maximum number of edge points; thus, a large number of circumferential pixels lying on the iris will pass through a common centre. The highest value in the accumulator gives the three coordinates (centre, radius) of the pupil–iris boundary. After this, the zigzag collarette area is detected which is concentric to the pupil and contains enough textural information.

2.2 Iris Normalization

For iris template matching, the segmented samples are normalized into fixed dimensions as these may vary with illumination changes and distance variation during acquisition. Daugman's rubber sheet model [12] is used which transforms iris image coordinates into polar coordinates. The iris segmentation and normalization results are shown in Fig. 2.

2.3 Feature Extraction

The feature extraction for iris texture is done using rotation-invariant and noise resistant Zernike moments (ZMs) [13] and polar complex exponential transform (PCET), polar cosine transform (PCT) and polar sine transform (PST) grouped under polar harmonic transforms (PHTs) [14] for NIR and visible iris samples. Both ZMs and PHTs have orthogonal kernels which give compact information by projecting the image onto a set of pair-wise orthogonal axes that limit the information redundancy. The image is mapped on a unit circle and is decomposed into a set of orthogonal kernels. Depending upon the moment order, the image is represented in terms of kernels which give real-valued features for further classification. As the order increases, more number of features get added which helps in discriminating between different classes. Thus, the purpose is to extract sufficient features which can provide adequate information for classifying the image. As the database consists of a large number of classes, the feature-set comprising ZMs and PHTs has the capability of generating sufficient invariant features. Though PCT, PST and PCET belong to PHT, all of these capture different image information. PHTs are easily computed without numerical instabilities at higher orders as opposed to ZMs which involve factorial terms for computation. After getting normalized iris samples of size 512×64, 32 patches of iris regions with an equal size of 32×32 without any overlapping are taken as shown in Fig. 1. Thus, at each of the 32 localized iris regions, the feature values are calculated till 15th order which makes 32 localized regions $\times 71$ features till 15th order = 2272 features of each of the four transforms used as illustrated in Table 1.

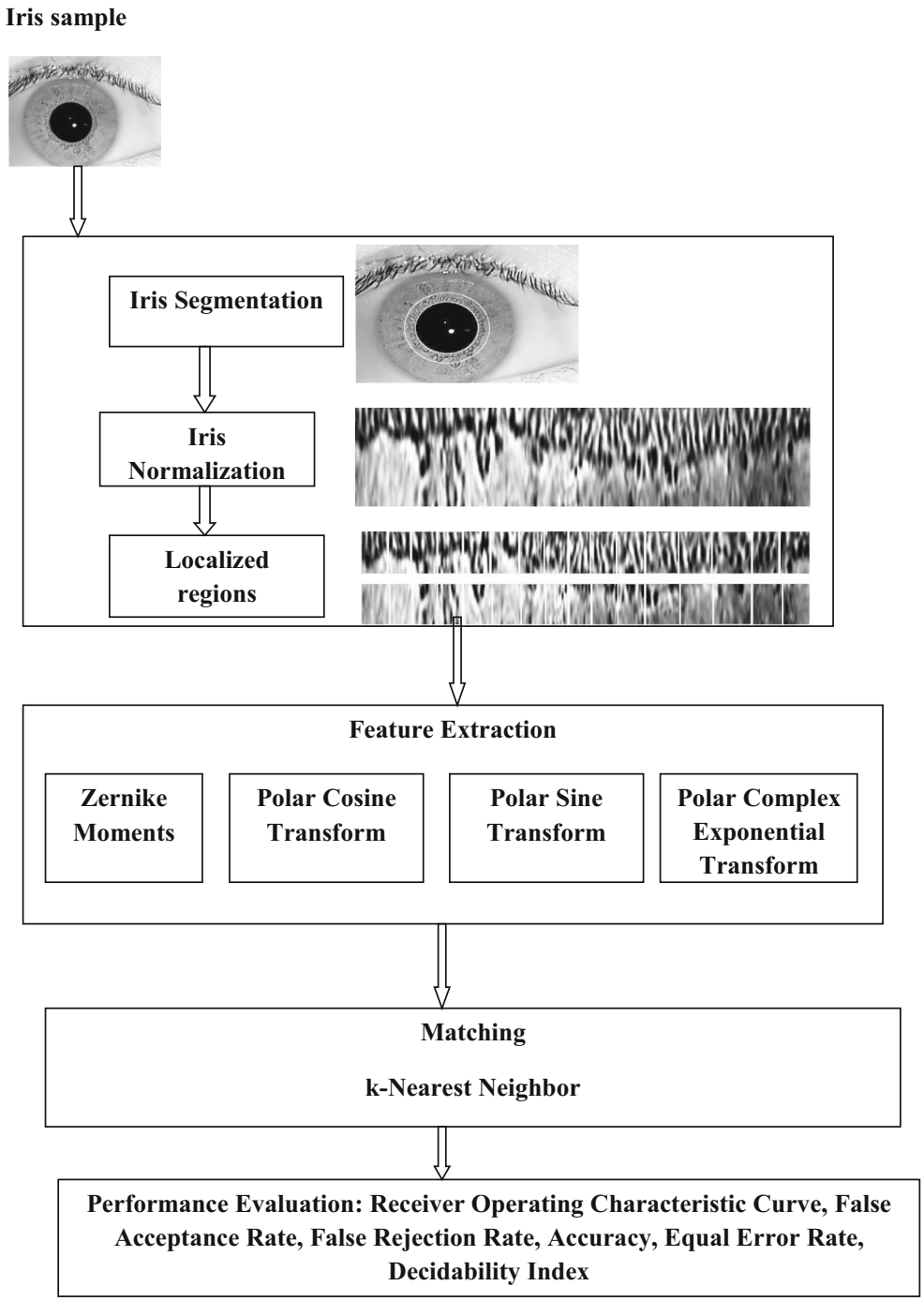

Fig. 1 Proposed iris recognition system

2.4 Classification

For iris template matching, *k*-nearest neighbor (k-NN) classifier is used which works well with noisy data comprising of a large number of classes. The classifier works on the principle which is based on minimum distance calculation between training and query samples based on the value '*k*' giving no. of neighbors. The invariant feature-set used for recognizing different classes works best with this classifier as it contains features which are highly correlated with the class yet are uncorrelated with one another. Simulations for all the five databases have been performed using distance metrics: Euclidean (ED), Manhattan (MD) and Chebyshev (CD) at '*k*' = 1, 2, 3, 4, 5. The results have been discussed in Sect. 3.2.

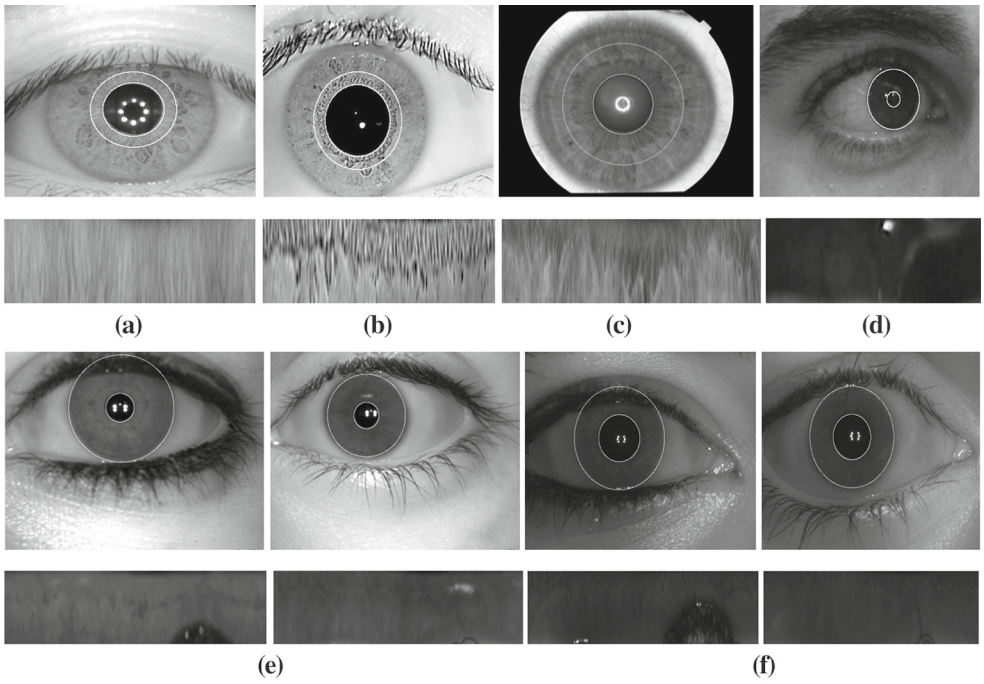

Fig. 2 Segmented and normalized iris samples of **a** CASIA-IrisV4-Interval, **b** IITD.v1, **c** UPOL, **d** UBIRIS.v2, **e** IIITD-CLI using CIS-202 dual iris sensor, **f** IIITD-CLI using VistaFA2E single iris sensor

Table 1 ZM and PHT feature-set

Order	ZMs/PHTs	No. of features	Accumulative
1	$M_{1,1}$	1	1
2	$M_{2,0}$; $M_{2,2}$	2	3
3	$M_{3,1}$; $M_{3,3}$	2	5
...			
15	$M_{15,1}$; $M_{15,3}$; $M_{15,5}$; $M_{15,7}$; $M_{15,9}$; $M_{15,11}$; $M_{15,13}$; $M_{15,15}$	8	71

3 Results and Discussion

The experiments have been conducted on MATLAB R2014a using Intel(R) Pentium(R) laptop with windows 7, 32-bit operating system at 2GHz with 4GB RAM memory.

3.1 Databases

For performance evaluation of the proposed method, five benchmark iris databases have been used: CASIA-IrisV4-Interval [15], IITD.v1 [16], UPOL [17], UBIRIS.v2 [18] and IIITD-CLI [19,20]. Extensive experiments have been performed on randomly selected subsets of the five publicly available databases. For CASIA-IrisV4-Interval and IITD.v1, a subset of 1500 randomly selected images of 150 subjects with 10 iris samples (5 left and 5 right iris) of each subject has been used. In case of UPOL, the entire database consisting of 384 images of 64 subjects with 6 iris samples of each subject has been employed. For UBIRIS.v2, a subset of 1700 iris images of 170 subjects with 10 samples (5 left and 5 right iris) of each subject has been utilized. In case of IIITD-CLI, the database consisting of iris samples without contact lenses has been used for 101 subjects with 10 samples (5 left and 5 right iris) each acquired from two sensors: CIS 202 and VistaFA2E. For comparison of the proposed approach with other techniques available in the literature, the databases have been divided into 60:40 training–testing ratio with equal or more number of randomly selected subsets following the same training–testing protocol as done by most of the existing techniques for fair performance evaluation.

3.2 Performance Evaluation of the Proposed Technique

The proposed technique is evaluated using performance indices: receiver operating characteristic curve (ROC), accuracy, false acceptance rate (FAR), false rejection rate (FRR), genuine acceptance rate, equal error rate (EER) and decidability index (DI) [21].

From Table 2, it can be deduced that the best recognition accuracy for all the databases is observed using Manhattan distance at 'k' = 1.

Figure 3 shows that PCET maintains a high classification rate. The proposed scheme is compared on various databases

Table 2 Recognition accuracy of iris databases using *k*-NN nearest neighbor

Value of '*k*'	*k*-NN using Manhattan				*k*-NN using Euclidean				k-NN using Chebyshev			
	ZM	PCT	PST	PCET	ZM	PCT	PST	PCET	ZM	PCT	PST	PCET
CASIA-IrisV4-Interval for 150 subjects												
1	**95.2**	**95.4**	**95.5**	**95.8**	94.5	94.6	94.8	95.2	92.1	92.5	92.9	93.5
2	92.7	92.8	92.8	93.2	91.6	91.9	92.3	92.5	90.2	90.5	90.6	90.7
3	91.6	91.7	91.8	91.8	89.5	89.6	89.6	89.7	88.4	88.6	88.7	88.7
4	85.7	85.9	86.4	86.5	84.6	84.8	85.0	85.0	80.3	80.4	80.7	80.9
5	79.4	79.5	79.7	79.8	78.5	78.8	78.9	78.9	75.6	75.9	76.4	76.8
IITD v1 for 150 subjects												
1	**96.4**	**96.5**	**96.6**	**96.7**	95.3	95.5	95.7	95.8	93.5	93.5	93.9	94.0
2	95.3	95.4	95.4	95.6	93.3	93.5	93.7	93.9	92.2	92.5	92.7	92.7
3	93.6	93.6	93.7	93.8	90.5	90.5	90.7	90.7	89.3	89.5	89.7	89.7
4	89.7	89.7	89.8	89.8	85.6	85.7	85.7	85.9	84.3	84.5	84.7	84.9
5	84.4	84.5	84.7	84.8	83.5	83.8	83.8	83.9	80.6	80.7	80.8	80.8
UPOL for 64 subjects												
1	**99.4**	**99.6**	**99.8**	**100**	98.3	98.5	98.7	98.7	97.2	97.5	97.9	98.2
2	98.3	98.4	98.5	98.7	97.1	97.3	97.7	97.8	96.5	96.5	96.7	96.8
3	95.6	95.6	95.7	95.8	93.2	93.5	93.6	93.7	92.4	92.5	92.6	92.7
4	91.7	91.8	91.8	91.8	90.5	90.7	90.7	90.8	89.3	89.4	89.5	89.6
5	89.5	89.7	89.8	89.8	88.5	88.6	88.7	88.7	85.6	85.7	85.7	85.8
UBIRIS v2 for 170 subjects												
1	**94.5**	**94.5**	**94.6**	**94.8**	93.1	93.5	93.7	93.7	91.0	91.4	91.9	91.9
2	90.0	90.4	90.4	90.8	89.2	89.5	89.6	89.7	87.2	87.5	87.7	87.7
3	88.5	88.6	88.7	88.8	85.0	85.5	85.7	85.7	84.2	84.5	84.7	84.8
4	85.2	85.6	85.6	85.7	82.1	82.5	82.8	82.8	81.3	81.4	81.4	81.7
5	82.2	82.5	82.7	82.8	80.3	80.5	80.6	80.9	79.2	79.7	80.1	80.2
IIITD-CLI (without lens) for 101 subjects												
1	**90.2**	**90.5**	**90.5**	**90.7**	89.1	89.5	89.6	89.7	86.2	86.4	86.8	86.9
2	85.0	85.3	85.4	85.5	84.2	84.5	84.5	84.7	82.2	82.5	82.7	82.9
3	78.5	78.8	78.8	78.9	75.0	75.5	75.6	75.6	73.2	73.5	73.7	73.7
4	70.2	70.4	70.5	70.5	68.1	68.5	68.6	68.7	66.3	66.4	66.6	66.8
5	63.0	63.3	63.5	63.6	61.2	61.2	61.3	61.5	60.0	60.2	60.2	60.6

Bold values indicate highest value of recognition accuracy for a particular feature-set

with recent approaches by quoting results from the respective papers as shown in Tables 3, 4 and 5.

For CASIA-IrisV4-Interval database, PCET gives an accuracy of 99.20% with EER as low as 0.01 and a high DI value of 4.70. For IITD.v1 database, PCET achieves best recognition accuracy of 99.85% with zero FAR, EER and DI of 4.75. For UPOL database, 100% accuracy is obtained in case of PCET with zero EER, FAR and FRR. For UBIRIS.v2 database, PCET shows an accuracy of 94.80% with DI = 2.82 and EER = 0.10 giving encouraging results as compared to recent methods which use lesser number of subjects. In case of IIITD-CLI, PCET achieves superior results with an accuracy of 90.70%, DI = 1.98 and EER = 8.11.

Table 6 shows that the computation of PHT kernels takes much lesser time as compared to ZM kernels when evaluated on a 32×32 normalized iris sample.

Textures contain high degree of randomness and irregularities; therefore, extracting a feature-set from localized region of interest (ROI) to characterize variations in intensity distribution proves to be effective rather than extracting features from the whole iris region which is more suitable for well-defined and deterministic spatial attributes. A feature-set constructed from Zernike polynomials and Polar Harmonic Transforms extracted from local 32×32 iris regions can effectively represent local intensity variations of iris texture. Therefore, the orthogonal moment-based invariant feature-set representing local intensity variations works best in discriminating between iris texture patterns of different subjects. Hence, the performance of the proposed technique is outstanding on all the databases used in this work and outperforms existing approaches.

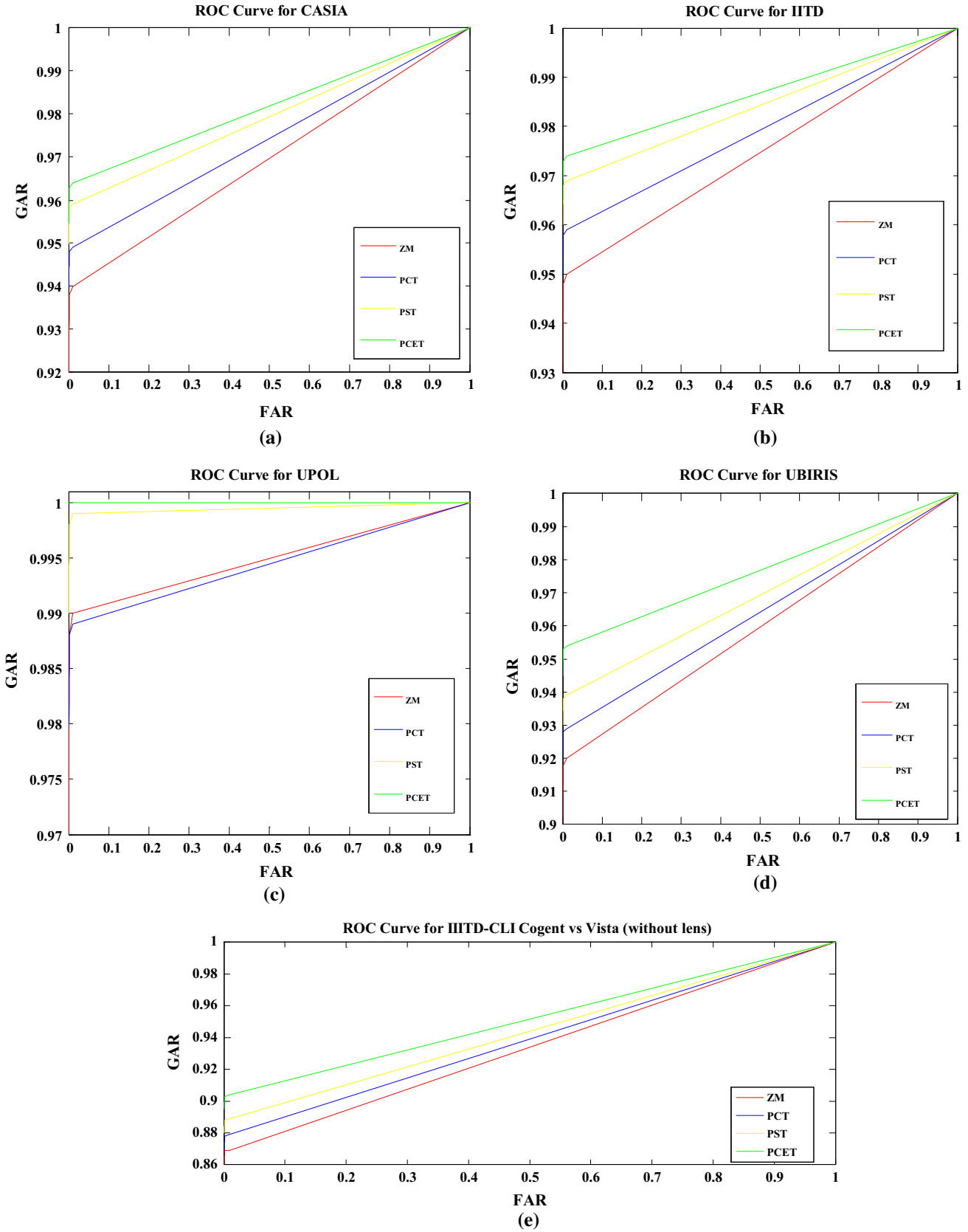

Fig. 3 ROC curves of **a** CASIA-Iris V4-Interval, **b** IITD.v1, **c** UPOL, **d** UBIRIS.v2, **e** IIITD-CLI database for Cogent versus Vista normal (without lens) iris samples

Table 3 Comparison of proposed method on CASIA-Iris V4-Interval and IITD.v1 with recent approaches

Database	Parameters	Log-Gabor filter [18]	*k*-nearest subspace [18]	Holistic subpattern [18]	Wavelet transform [18]	Wavelet transform [18]	Triplet half-band filter [8]	Discrete Wavelet Transform [11]	ZM	PCT	PST	PCET
CASIA-IrisV4-Interval	Subjects	108	60	80	108	100	–	–	150	150	150	150
	Matching	Hamming distance	Cumulative sparse concentration index (CSCI)	MD	Particle swarm optimization+ probabilistic neural network	Euclidean distance	–	–	MD	MD	MD	MD
	Training images per subject	–	3	2	3	–	–	–	6	6	6	6
	Testing images per subject	–	1	2	4	–	–	–	4	4	4	4
	FAR (%)	0.01	0.56	–	0.01	–	–	–	0.00	0.00	0.00	0.00
	FRR (%)	0.24	13.30	–	0.64	–	–	–	4.80	4.60	4.50	4.20
	Accuracy (%)	99.75	99.43	97.50	99.35	98.91	–	–	95.20	95.40	95.50	95.80
	EER	–	–	–	–	–	–	–	0.39	0.22	0.14	0.11
	DI	6.20	–	–	–	–	–	–	1.12	1.45	1.67	1.98
IITD.v1	Subjects	–	100	–	–	–	90	80	150	150	150	150
	Matching	–	CSCI	–	–	–	*k*-out-n post-classifier	*k*-NN	MD	MD	MD	MD
	Training images per subject	–	4	–	–	–	2	–	6	6	6	6
	Testing images per subject	–	1	–	–	–	3	–	4	4	4	4
	FAR (%)	–	0.70	–	–	–	0.16	–	0.00	0.00	0.00	0.00
	FRR (%)	–	12.00	–	–	–	0.15	–	3.60	3.50	3.40	3.30
	Accuracy (%)	–	99.20	–	–	–	99.84	99.50	96.40	96.50	96.60	96.70
	EER	–	–	–	–	–	–	0.04	0.06	0.04	0.02	0.01
	DI	–	–	–	–	–	–	–	3.13	4.38	4.45	4.53

Table 4 Comparison of proposed method on UPOL and IIITD-CLI with recent approaches

Database	Parameters	Curvelet transform [22]	Color space histogram [23]	Complex steerable pyramid [24]	Coiflet wavelet transform [25]	Haar, symlet, biorthogonal [26]	Morphological features [6]	Real-valued Log-Gabor phase [27]	mLBP [19]	ZM	PCT	PST	PCET
UPOL	Subjects	64	64	64	64	64	64	–	–	64	64	64	64
	Matching	Correlation coefficient	Cross-correlation	Fusion rules	Hamming distance	Absolute difference	SVM fusion	–	–	MD	MD	MD	MD
	Training images per subject	4	2	4	3	3	–	–	–	4	4	4	4
	Testing images per subject	1	4	2	2	2	–	–	–	2	2	2	2
	FAR (%)	–	–	–	–	–	–	–	–	0.00	0.00	0.00	0.00
	FRR (%)	–	–	–	–	–	–	–	–	0.60	0.40	0.20	0.00
	Accuracy (%)	97.80	100	100	82.90	95.90	100	–	–	99.40	99.60	99.80	100
	EER	0.05	0.00	0.00	0.28	0.04	0.01	–	–	0.04	0.01	0.00	0.00
	DI	–	–	–	–	–	–	–	–	4.66	4.67	4.74	4.84
IIITD-CLI (without lens)	Subjects	–	–	–	–	–	–	101	101	101	101	101	101
	Matching	–	–	–	–	–	–	DA-NBNN	–	MD	MD	MD	MD
	Training images per subject	–	–	–	–	–	–	–	–	6	6	6	6
	Testing images per subject	–	–	–	–	–	–	–	–	4	4	4	4
	FAR (%)	–	–	–	–	–	–	–	–	0.20	0.17	0.17	0.14
	FRR (%)	–	–	–	–	–	–	–	–	9.80	9.50	9.50	9.30
	Accuracy (%)	–	–	–	–	–	–	89.92	72.96	90.20	90.20	90.50	90.70
	EER	–	–	–	–	–	–	10.02	–	8.90	8.34	8.20	8.11
	DI	–	–	–	–	–	–	–	–	1.56	1.89	1.90	1.98

Table 5 Performance comparison of UBIRIS.v2 database with recent approaches

References	Feature extraction	Subjects	Matching	Training images per subject	Testing images per subject	FAR (%)	FRR(%)	Accuracy (%)	EER	DI
[28]	Gabor filter	80	Possibilistic fuzzy matching	3	2	–	–	97.11	7.80	–
[10]	Gabor features	151	Bayesian fusion	5	1–2	–	–	–	0.19	1.58
[10]	Ordinal features	151	Personalized weight map matching	5	1–2	–	–	–	0.26	1.37
[10]	Log-Gabor	151	Fractional hamming	5	1–2	–	–	–	0.25	1.09
[10]	2D phase-based discrete Fourier transform	151	Hamming distance	5	1–2	–	–	–	0.40	0.45
[10]	Log-Gabor and Zernike moments	151	Phase distance	5	1–2	–	–	–	0.12	2.57
Proposed	Zernike moments	170	Manhattan	6	4	0.14	5.50	94.50	0.12	2.73
Proposed	PCT	170	Manhattan	6	4	0.14	5.50	94.50	0.12	2.73
Proposed	PST	170	Manhattan	6	4	0.12	5.40	94.60	0.11	2.78
Proposed	PCET	170	Manhattan	6	4	0.11	5.20	94.80	0.10	2.82

Table 6 Computation time of the proposed iris recognition system

Proposed method	Computation time (in seconds)
Iris segmentation (CHT)	2.67
Iris normalization	0.23
ZM	4.89
PCT	2.76
PST	1.78
PCET	2.13
Matching (training)	0.04
Matching (testing)	2.78

4 Conclusion

In this paper, a feature-set consisting of Zernike moments and Polar Harmonic Transforms with invariance to rotation, noise and illumination proves to be effective for cross-domain iris recognition. The features are calculated till 15th order at localized iris regions on five benchmark databases: CASIA-IrisV4-Interval, IITD.v1, UPOL, UBIRIS.v2 and IIITD-CLI. Experiments demonstrate that the proposed method outperforms state-of-the-art methods in terms of accuracy, FAR, FRR, EER and DI. In future, more modalities can be used to make an effective biometric system.

Acknowledgements The authors acknowledge Chinese Academy of Sciences-Institute of Automation (CASIA), China, Indian Institute of Technology, Delhi (IITD), University of Palack'eho and Olomouc and Soft Computing and Image Analysis Group (SOCIA Lab.), Department of Computer Science, University of Beira Interior, Covilhã, Portugal and Indraprastha Institute of Information and Technology, Delhi (IIITD), for providing iris databases used in this work. The authors are also grateful to anonymous reviewers for their constructive comments which improved the quality of the manuscript.

References

1. UID Authority of India.: Role of biometric technology in Aadhaar enrollments. http://uidai.gov.in/images/FrontPageUpdates/role_of_biometric_technology_in_aadhaar_jan21_2012.pdf (2012)
2. Tan, C.W.; Kumar, A.: Adaptive and localized iris weight map for accurate iris recognition under less constrained environments. In: Proceedings of the IEEE 6th International Conference on Biometrics, Theory Application System (BTAS), pp. 1–7
3. Daugman, J.: High confidence visual recognition of persons by a test of statistical independence. IEEE Trans. Pattern Anal. Mach. Intell. **15**(1), 1148–1161 (1993)
4. Bhateja, A.K.; Sharma, S.; Chaudhury, S.; Agrawal, N.: Iris recognition based on sparse representation and k-nearest subspace with genetic algorithm. Pattern Recogn. Lett. **73**, 13–18 (2016)
5. Liu, Y.; He, F.; Zhu, X.; Liu, Z.; Chen, Y.; Han, Y.; Yu, L.: The improved characteristics of bionic gabor representations by combining with sift key-points for iris recognition. J. Bionic Eng. **12**(3), 504–517 (2015)
6. Umer, S.; Dhara, B.C.; Chanda, B.: Iris recognition using multiscale morphologic features. Pattern Recogn. Lett. **65**, 67–74 (2015)

7. Rai, H.; Yadav, A.: Iris recognition using combined support vector machine and Hamming distance approach. Expert Syst. Appl. **41**(2), 588–593 (2014)
8. Umer, S.; Dhara, B.C.; Chanda, B.: A novel cancelable iris recognition system based on feature learning techniques. Inf. Sci. **406**, 102–118 (2017)
9. Alvarez-Betancourt, Y.; Garcia-Silvente, M.: A keypoints-based feature extraction method for iris recognition under variable image quality conditions. Knowl. Based Syst. **92**, 169–182 (2016)
10. Tan, C.W.; Kumar, A.: Accurate iris recognition at a distance using stabilized iris encoding and Zernike moments phase features. IEEE Trans. Image Process. **23**(9), 3962–3974 (2014)
11. Masek, L.: Recognition of human iris patterns for biometric identification, pp. 1–7. http://www.csse.uwa.edu.au/opk/studentprojects/labor (2003)
12. Daugman, J.: How iris recognition works. IEEE Trans. Circuits Syst. Video Technol. **14**(1), 21–30 (2004)
13. Teague, M.R.: Image analysis via the general theory of moments. J. Opt. Soc. Am. **70**(8), 920–930 (1980)
14. Yap, P.T.; Jiang, X.D.; Chung, A.C.: Two-dimensional polar harmonic transforms for invariant image representation. IEEE Trans. Pattern Anal. Mach. Intell. **32**(7), 345–351 (2010)
15. CASIA Iris Image Database. http://biometrics.idealtest.org
16. Kumar, A.; Passi, A.: Comparison and combination of iris matchers for reliable personal authentication. Pattern Recogn. **43**(3), 1016–1026 (2010)
17. Dobes, M.; Machala, L.: Iris database, Palacky University in Olomouc, Czech Republic. http://www.inf.upol.cz/iris (2007)
18. Proenca, H.; Filipe, S.; Santos, R.; Oliveira, J.; Alexandre, L.A.: The UBIRIS.v2: a database of visible wavelength iris images captured on the move and at-a-distance. IEEE Trans. Pattern Anal. Mach. Intell. **32**(8), 1529–1535 (2010)
19. Yadav, D.; Kohli, N.; Doyle, J.; Singh, R.; Vatsa, M.; Bowyer, K.: Unraveling the effect of textured contact lenses on Iris recognition. IEEE Trans. Inf. Forensics Secur. **9**(5), 851–862 (2014)
20. Kohli, N.; Yadav, D.; Vatsa, M.; Singh, R.: Revisiting Iris Recognition with Color Cosmetic Contact Lenses. In: Proceedings of the 6th IAPR, pp. 1–5 (2013)
21. Dong, W.; Sun, Z.; Tan, T.: Iris matching based on personalized weight map. IEEE Trans. Pattern Anal. Mach. Intell. **33**(9), 1744–1757 (2011)
22. Patil, C.M.; Patilkulkarani, S.: An approach of iris feature extraction for personal identification. In: International Conference on Advances in Recent Technologies in Communication and Computing, pp. 796–799 (2009)
23. Rahulkar, A.D.; Holambe, R.S.: Half iris feature extraction and recognition using a new class of biorthogonal triplet half-band filter bank and flexible k-out-of-n: a postclassifier. IEEE Trans. Inf. Forens. Secur. **7**(1), 230–240 (2012)
24. Elgamal, M.; Al-Biqami, N.: An efficient feature extraction method for iris recognition based on wavelet transformation. Int. J. Comput. Inf. Technol. **2**(3), 521–527 (2013)
25. Ahamed, A.; Bhuiyan, M.I.H.: Low complexity iris recognition using curvelet transform. In: IEEE Proceedings of the International Conference on Informatics, Electronics and Vision, pp. 548–553 (2012)
26. Demirel, H.; Anbarjafari, G.: Iris recognition system using combined histogram statistics. In: Proceedings of the IEEE International Symposium on Computer and Information Sciences, pp. 1–4 (2008)
27. Gragnaniello, D.; Poggi, G.; Sansone, C.; Verdoliva, L.: An investigation of local descriptors for biometric spoofing detection. IEEE Trans. Inf. Forensics Secur. **10**(4), 849–863 (2015)
28. Ross, A.; Sunder, M.S.: Block based texture analysis for iris classification and matching. In: IEEE Proceedings of the Workshops on Computer Vision and Pattern Recognition, pp. 30–37 (2010)